ACOUSTICS IN OPTICAL FIBRES: A HARMONIOUS COLLABORATION OF SOUND AND LIGHT

G. KAKARANTZAS, A.DIEZ, T.A. BIRKS AND P.ST.J. RUSSELL

OPTOELECTRONICS GROUP, DEPARTMENT OF PHYSICS, UNIVERSITY OF BATH

CLAVERTON DOWN, BATH BA2 7AY, UNITED KINGDOM

1. INTRODUCTION

Photoelasticity is the change of refractive index of a solid due to mechanical stress. This phenomenon makes possible the acousto-optic effect-the interaction of acoustic and optical waves-in which an acoustic wave launched by means of a piezoelectric transducer, produces a periodic refractive index change in the solid. This interaction between light and sound becomes very interesting in optical fibres. Periodic micro-bends generated by flexural acoustic waves create the equivalent a of "long period grating",and highly efficient coupling between different optical modes of the fibre occurs. This interaction has been used to demonstrate a number of all-fibre devices such as frequency shifters, filters and optical switches. These could be greatly improved if techniques were developed to control the propagation of the flexural waves, much as the optical waves can already be controlled. Hence, we have developed acoustic Bragg gratings in narrowed optical fibres, and have combined them to create an acoustic cavity. The acoustic Bragg grating is formed by a chain of biconical microtapers, that modulate periodically the fibre diameter and hence the forward wave velocity, and it exhibits a frequency stop-band for flexural acoustic waves. The acoustic cavity is formed from two such reflectors. The flexibility of the fabrication technique, employing a CO_2 laser as a heat source, readily allows changes to the parameters involved, thus making it possible to shift the centre frequency and adjust the width of the acoustic stop band. Such structures are suitable as frequency-selective acoustic mirrors in acousto-optic fibre devices. In this paper, the physics of these interactions together with some recent results and potential applications will be discussed and reviewed.

2. ACOUSTO-OPTIC INTERACTION IN OPTICAL FIBRES: DEMONSTRATION OF A TUNABLE, NARROW BAND ACOUSTO-OPTIC FILTER.

With the proliferation of wavelength division multiplexing, the development of methods for dynamic routing and filtering on a per-wavelength basis is becoming increasingly important. Tunable filters and wavelength selective switches with low optical loss and narrow bandwidth are required. One class of device with potential to address this problem is the all fibre acousto-optic tunable filter (AOTF). These devices use acoustically induced mode coupling in fibre to perform switching or filtering functions. Because they are fabricated entirely from fibre they can have extremely low insertion loss and, therefore, offer the possibility of being used in switching nodes where they could be concatenated without the need for intermediate amplifiers.

Devices of this type have been used as notch filters [1-3] frequency shifters [4], and wavelength selective switches [5]. They have been fabricated from single mode fibre, two-mode fibre, tapered fibre, or fused fibre couplers.

Narrow spectral width is difficult to achieve for a variety of reasons. For devices based on standard diameter (not tapered) fibre, the requirement that the acoustic energy couple efficiently to the core of the fibre limits the maximum acoustic frequency so that narrow bandwidths can only be achieved with very long interaction lengths [1,2]. By tapering the optical fibre, shorter acoustic wavelengths can be obtained and narrow band devices of practical length are possible. Never the less, because of the difficulty associated with producing sufficiently uniform tapers, narrow bandwidth tapered fibre AOTFs have only recently been demonstrated [6].

A schematic diagram of the tapered fibre, AOTF is shown in Fig. 1. The filter functions as follows: When driven with an rf signal, a piezoelectric transducer produces an acoustic vibration that is amplified and transmitted to the optical fibre by a glass horn. The horn can be coaxial with the fibre (as shown in Fig. 1) or can be attached from the side. The acoustic wave propagates as a flexural wave along the fibre where it is further amplified by the fibre taper transition. The flexural wave achieves its maximum amplitude at the taper waist. Light entering the tapered region of the fibre spreads out of the fibre core exciting the fundamental (HE_{11}) mode of the taper waist. In the absence of a resonant acoustic wave this light travels through the taper waist undisturbed and is captured by the fibre core as it propagates up the taper transition. When an acoustic wave is present, periodic microbends in the taper waist couple light of the resonant wavelength(s) from the HE_{11} mode to one or more higher order modes. The higher order modes are not captured by the fibre core at the far end of the taper and are rapidly stripped by the buffer coating. Notches in the

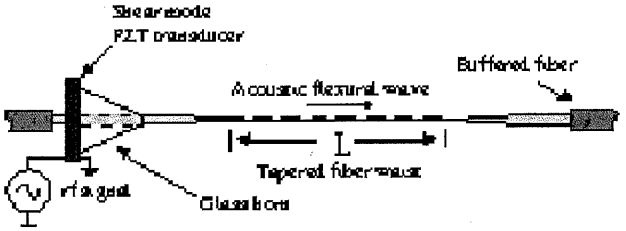

Fig. 1. Schematic diagram of tapered fibre acousto-optic tunable filter.

optical spectrum of the output light appear at wavelengths for which the acoustic wavelength, Λ, satisfies the resonance condition

$$\Lambda = \frac{2\pi}{\beta_0 - \beta_n} \qquad (1)$$

In Eq. 1. β_0 is the propagation constant of the HE_{11} mode and β_n is the propagation constant of the nth higher order mode.

In this work, coupling between the HE_{11} and the next three (TE_{01}, HE_{21}, TM_{01}) modes was obtained. In untapered fibre, these three modes are nearly degenerate and sum to form the LP_{11} modes. However, as the fibre is tapered to small diameters the splitting becomes significant and the LP approximation is no longer valid. Analysis shows that the coupling efficiency to the TM_{01} and the TE_{01} modes is polarization dependent but coupling to the HE_{21} mode is independent of the state of polarization of the input light.

In order to obtain a narrow spectral width and a clean notch shape it is critical that phase matching be maintained over the entire length of the taper waist. This means that the taper diameter must be highly uniform throughout its length since both the modal dispersion and the acoustic wavelength vary with the taper diameter. As the diameter of a fibre is reduced through tapering, the resonant acoustic wavelengths (given by Eq. 1) change because the propagation constants change. When tapering extends beyond the point at which the fundamental mode is guided by the cladding-air interface, the difference between propagation constants increases and

the resonant acoustic wavelength drops significantly. This results in a reduction of the bandwidth-length product. This behavior is shown in Fig. 2 for coupling between the fundamental HE_{11} mode and the HE_{21} mode. Fig. 2 illustrates the fact that very small bandwidth-length products can be obtained in tapered fibre devices.

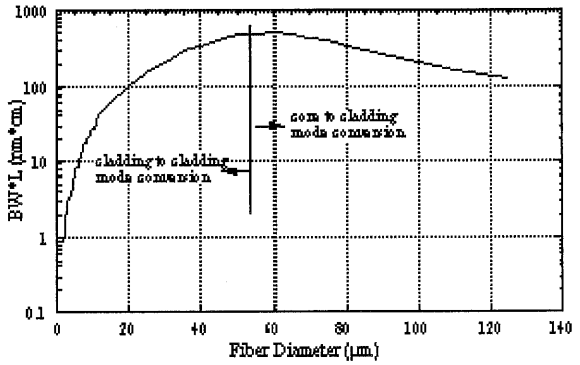

Fig. 2. Bandwidth-length product as a function of fibre taper waist diameter for coupling from the HE_{11} to the HE_{21} mode.

We have developed a fibre taper fabrication rig capable of producing fibre tapers with waist uniformity better than +/- 0.1%. Using this rig we have produced tapered fibre acousto-optic notch filters of various taper diameters and notch bandwidths. The transmission spectrum of the narrowest bandwidth filter we obtained is shown in Fig. 3. The filter was tested using an erbium-doped fibre ASE source and an optical spectrum analyzer. It had a taper diameter of 6.1 μm and a waist length of 4 cm. The total length of the filter unit including the taper transitions and the transducer was less than 10 cm. The excess loss was 0.02 dB and the maximum extinction was greater than 20 dB (limited by the resolution of the OSA). The acoustic frequency corresponding to an HE_{21} notch wavelength of 1550 nm was 7.7 MHz. The center wavelength of the notch could be tuned by adjusting the acoustic frequency.

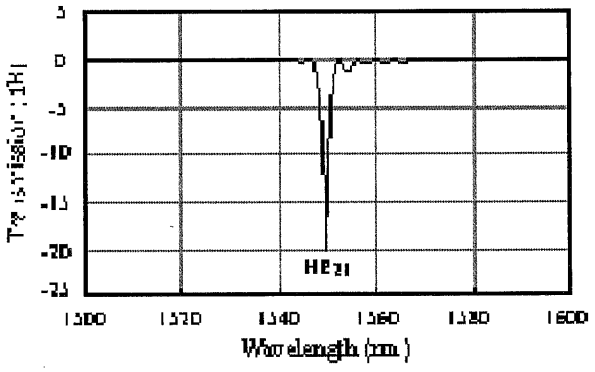

Fig. 3. Transmission spectrum of a tapered fibre AOTF with a 6.1 μm waist diameter and a 4 cm long interaction length.

The smallest bandwidth-length product we obtained was 6.4 nm*cm. This was achieved by a device with a taper waist diameter of 4.2 μm. This filter had a bandwidth of 3.2 nm and a taper waist length of 2 cm. The tuning characteristic of this filter is shown in Fig. 4. Indicated on the figure are curves for the TE_{01} and TM_{01} notches as well as the HE_{21} notch. Because of the high frequency (27 MHz) at resonance, a $LiNbO_3$ transducer was required. PZT transducers were used in the other devices. Fig. 5 is a theoretical plot of the resonance wavelength of the three

lowest order modes as a function of taper diameter. For the plot, the acoustic frequency was chosen as a function of taper waist radius to obtain a constant resonant wavelength for the HE_{21} mode of 1550 nm. The notch separation (wavelength spacing between adjacent modes) increases as the taper diameter is reduced. For this reason the 4.2 μm diameter device provided the widest mode spacing. For this device the wavelength separation between the TE_{01} and HE_{21} resonances was 233 nm and the separation between the TM_{01} and HE_{21} resonances was 95 nm.

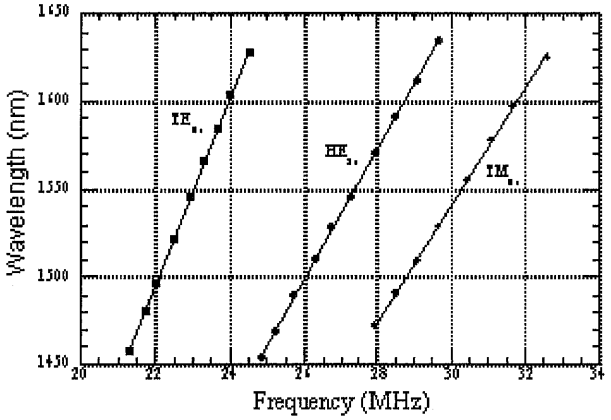

Fig. 4. Tuning of resonance wavelengths for coupling to the TM_{01}, HE_{21} and TE_{01} modes as a function of acoustic frequency for a 4.2 μm waist diameter filter

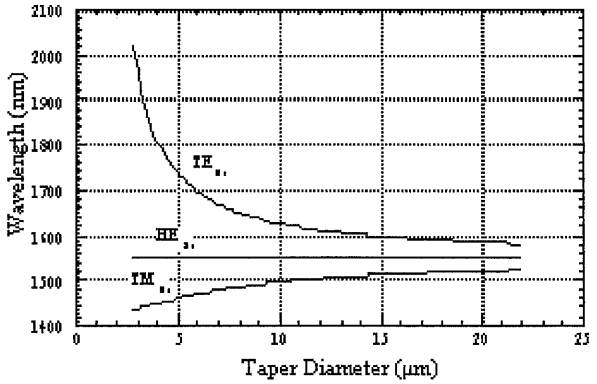

Fig. 5. Resonance wavelength as a function of taper waist diameter for coupling to the TE_{01}, HE_{21} and TM_{01} modes. The acoustic frequency is chosen to obtain a resonance wavelength for the HE_{21} mode of 1550 nm.

As was mentioned earlier, the depth of the HE_{21} notch is expected to be polarization insensitive but the TE_{01} and TM_{01} notch depth should vary with the state of polarization of the incoming light. This was verified experimentally by polarizing the output of the ASE source and placing a polarization controller in-line prior to the notch filter. Fig. 6 shows the transmission spectrum of a 7.5 μm diameter, 4 cm long notch filter. In Fig. 6a the polarization state was adjusted to maximize the depth of the TM_{01} notch. In Fig. 6b the polarization state was changed and the depth of the notch was reduced considerably. As expected, the depth of the HE_{21} notch did not change as the polarization state was varied.

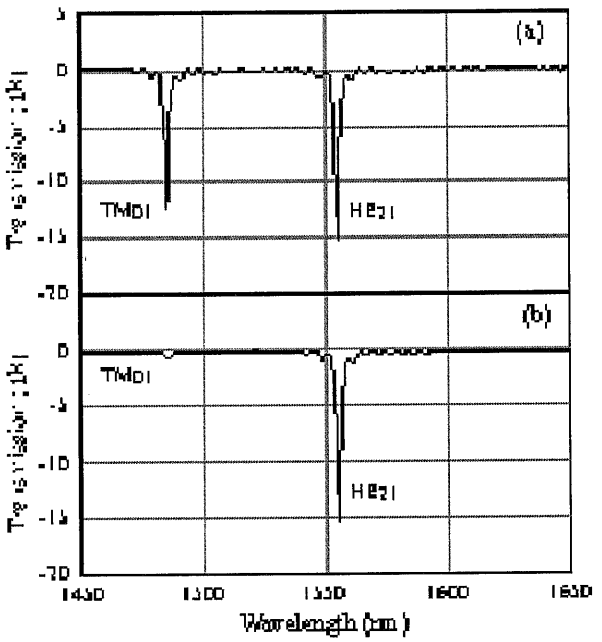

Fig. 6. Transmission spectrum of tapered fibre AOTF showing polarization insensitivity of HE_{21} notch. (a) Input polarization adjusted to maximize the depth of TM_{01} notch (b) Input polarization state changed to reduce the TM_{01} notch depth.

3. ACOUSTICS IN OPTICAL FIBRES

3.1 ACOUSTIC STOP BAND IN OPTICAL FIBRE PERIODIC MICROSTRUCTURES

In recent years the propagation of electromagnetic waves in artificial periodic structures of dielectric materials ("photonic crystals") has received great attention [7]. Appropriately designed structures can be opaque at all angles of incidence for electromagnetic waves within certain ranges of frequency. Because of the analogy between such behaviour and that of electrons in crystals, the forbidden frequency ranges have been called photonic band gaps. In these frequency ranges waves are evanescent because they are reflected by the structure. In principle, band gaps can appear when the wavelength of the electromagnetic wave approaches the period of the structure.

Since only waves and periodic scatterers are required to generate band gap phenomena, they are also possible for mechanical (acoustic) waves propagating in a periodic structure. Several theoretical works concerning acoustic band gaps in periodic media have been reported [8,9]. Recently, the first experimental study concerning ultrasonic band gaps was reported [10]; in this work, the authors report on sound attenuation experiments performed on a minimalistic sculpture. Acoustic band gaps have also been observed experimentally in different one-dimensional [11,12] and two-dimensional structures [13-16].

Here, we present a detailed study of a one-dimensional periodic microstructure - an acoustic Bragg grating - on an optical fibre. It consists of a number of concatenated and equally spaced biconical micro-tapers, giving a periodic modulation of the diameter along the fibre. Since the velocity of flexural acoustic waves in rods depends on the diameter of the rod, the structure behaves as the periodic concatenation of media with different impedances, so acoustic stop bands are expected. Moreover, it can be designed to be optically inactive over wide range of

wavelength ranges. Our interest in this kind of acoustic grating is motivated by its potential applications in optical fibre acousto-optic devices [12,13].

A recently reported fibre optic tapering technique [19] with a CO_2 laser was used to fabricate the periodic microstructure on a standard single-mode telecommunications fibre made from fused silica (outer diameter 125 μm). The fibre was first narrowed to a uniform diameter of 15 μm over a length of 30 mm by heating and stretching, forming a primary taper structure. One point in this section was then heated by exposure to the focused laser beam and elongated using two translation stages at very low speed, to form a secondary micro-taper structure. This secondary process was repeated several times at equally spaced intervals along the narrowed fibre. Part of the resulting structure is shown in Fig.7. The pitch is 300 μm, the minimum micro-taper diameter is 10 μm and the full structure has 56 periods. The total length of the periodic structure is 17 mm.

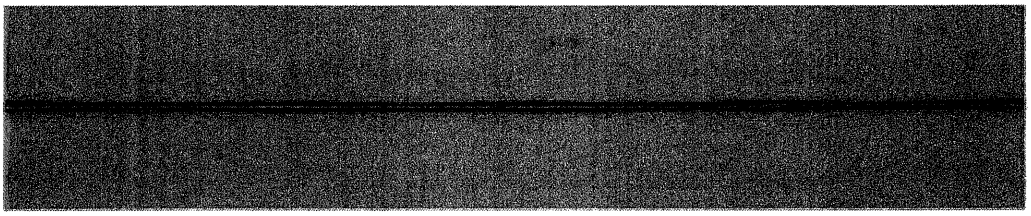

Figure 7.An optical micrograph of part of a similar periodic structure as the one used in the experiments.

Fig. 8 illustrates the experiment used to characterise the acoustic properties of the structure. Flexural acoustic waves were excited on the fibre by a fused silica horn attached to a thickness-mode piezoelectric transducer, which was driven by a radiofrequency electrical signal [12,13]. The acoustic wave propagates along the fibre and is concentrated by the primary taper transition, so large amplitudes can be imposed on the narrowed fibre and the acoustic grating.

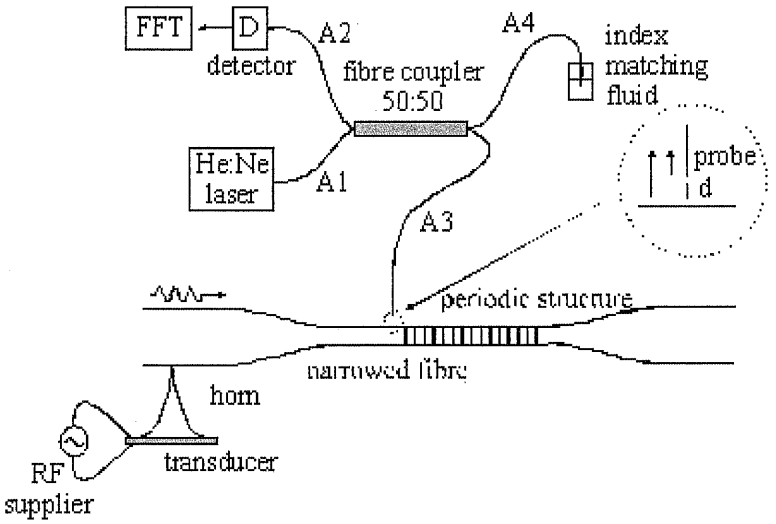

Figure 8. A schematic diagram (not to scale) of the experimental configuration, showing the acoustic grating structure and the optical vibrometer.

In general the acoustic grating works as a one-dimensional Bragg reflector, with a reflection coefficient that depends on frequency. Therefore, a resonant cavity is defined between it and the fixed point at the tip of the horn. For an acoustic signal with a frequency matched to one of the longitudinal resonances of the cavity, a standing wave is formed by the combination or

superposition the launched and reflected waves. Here, the length of this cavity was approximately 70 mm and so a large number of resonances were supported.

The amplitude of the acoustic wave at any point along the structure was measured using a sensitive interferometric optical fibre vibrometer [20], a diagram of which is included in Fig. 8. The cleaved end of a probe fibre carrying light from a He-Ne laser is positioned very close to the vibrating surface. Light is Fresnel-reflected back into the fibre by the fibre's end-face and by the external surface, which together form a low-finesse Fabry-Perot interferometer. The reflected light is detected and analysed by a digital oscilloscope with a fast Fourier transform-processing capability. It can be shown that the detected signal contains harmonics of the frequency of vibration of the surface, the relative amplitudes of which can be related to the amplitude of the vibration. Using this technique, acoustic amplitudes of less than 1 nm can be measured. Moreover, in the case of standing waves, the wavelength can be measured by scanning the probe along the vibrating surface.

Using the experimental apparatus described above, different measurements were carried out on the narrowed fibre. By positioning the probe between the acoustic grating and the horn and scanning it along the fibre, the standing wave ratio (SWR) at each longitudinal resonant frequency of the cavity between 0.1 and 1.4 MHz was measured, Fig. 9(a). There was a very well defined stop band centred at 0.8 MHz. SWRs as high as 55 dB were found, this value being limited by the sensitivity of the measurement system. The inset in Fig. 9(a) is a plot of acoustic amplitude versus position for a frequency the centre of the stop band, clearly showing the nodes and antinodes of a standing wave. The power transmission coefficient T was calculated from the SWR data (assuming no losses) and is shown in Fig. 9(b), the value of -22 dB in the stop band again being limited by the sensitivity of the measurement.

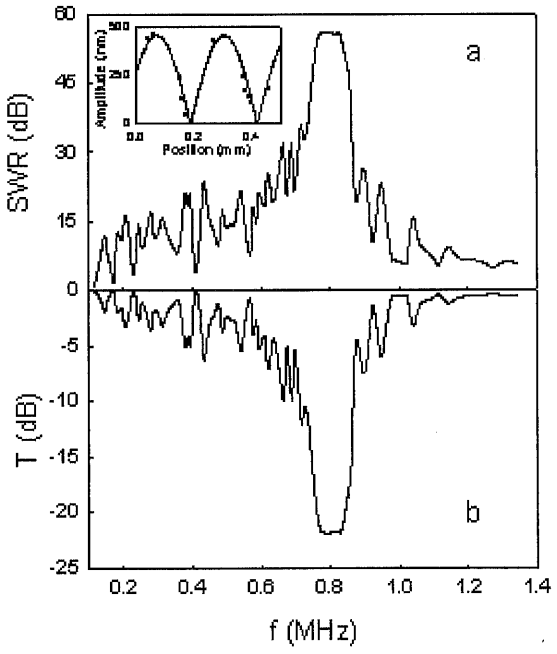

Figure. 9 a) SWR as a function of frequency. Inset: Standing wave shape for a frequency of 0.8 MHz. (b) Transmission spectrum calculated from the SWR.

No standing wave component was found when the probe was positioned beyond the acoustic grating, confirming that the reflection was due to the grating and not from any other source (such as the fibre holder). Direct measurement of T was not straightforward, but we could show that its value at the centre of the stop band was in fact less than -50 dB, once again limited by measurement sensitivity with no transmitted amplitude being measurable.

The vibrometer also allowed us to measure the amplitude of the vibration within the grating, so that the decay of acoustic waves along it could be measured. The inset of Fig. 10 shows the measured acoustic amplitude along a section of the grating for a frequency at the centre of the stop band. The decay of the standing wave is clearly defined. Successive maxima of the acoustic amplitude along the structure are plotted in Fig. 10 at a similar frequency. A section of the uniform narrowed fibre is included, where the maxima have a constant value. Then, within the grating, the rapid decay of the acoustic amplitude is evident. After thirty periods the amplitude falls below the resolution limit of the measurement system (1 nm), indicating that the device could be shortened and still function well as a reflector. An exponential fit to the data yields an attenuation factor of 5 dB/mm.

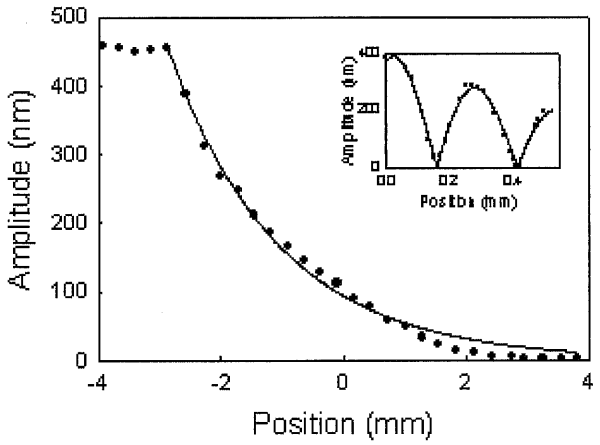

Figure 10. A plot of successive maxima of the acoustic amplitude along the narrowed fibre, for the frequency of 0.8 MHz at the centre of the stop band. Inset: Typical shape of the standing wave within the grating for a similar frequency.

3.2 1-D ACOUSTIC CAVITY IN OPTICAL FIBRES USING TWO ACOUSTIC BRAGG GRATINGS.

In the previous section we described the fabrication and acoustic properties of a one-dimensional periodic microstructure (an acoustic Bragg grating) made with optical fibre that had been tapered - narrowed by heating and stretching. Taking the process one step further, an acoustic cavity can be formed from two such reflectors. The cavity can be regarded as a single acoustic grating with a long defect in the middle. When a defect is introduced into a periodic structure, states localized around the defect appear at frequencies within the stop band, generating narrow transmission bands at those frequencies. From a more traditional point of view, the structure can also be seen as a simple resonator formed from two reflectors. In the frequency range where their reflectivity is high (the stop band of the gratings), the structure acts as a true resonator and so only certain frequencies are allowed to propagate inside the cavity, i.e. the longitudinal modes. Transmission peaks occur at these frequencies.

The acoustic cavity was fabricated from a standard telecommunication fibre by combining standard fibre optic tapering and a CO_2 laser based micro-tapering technique [19]. Two similar gratings were written, leaving the central part of the tapered fibre unchanged. The gratings both had 10 periods, the period was 285 μm and the minimum diameter was 10 μm. The length of the cavity between the gratings was 9 mm. The experimental setup used to characterize the acoustic cavity was similar to that described in the previous section.

The theoretical modeling of the structure was based on the scattering theory for transverse acoustic plane waves incident normally into a multilayer stack of elastic media [21]. The reflection and transmission coefficients can be expressed as functions of layer thicknesses and propagation constants within them, as well as material properties and frequency. We

approximated the structure by a number of cylindrical sections, each one having constant radius R. In the low frequency regime, higher order flexural modes are cut-off and only the fundamental flexural mode is allowed to propagate. Within each section, the propagation constant β of the fundamental flexural mode can be approximated by

$$\beta = \sqrt{\frac{4\pi f}{R\, c_{ext}}} \qquad (2)$$

where f is the frequency and c_{ext} is the speed of extensional waves (5760 ms^{-1} for fused silica). This expression assumes that the fibre is under no strain. Once the propagation constant of the wave at each region was obtained, the reflection and transmission coefficients of the whole structure were calculated. The gratings were divided in 200 sections per period, while the central gap was considered as a single section, ensuring 0.1% accuracy.

Figure 11(a) is the measured reflection spectrum of the full acoustic cavity. Within the stop band, which was over 150 kHz broad centred on ~850 kHz, several peaks are observed which correspond to the cavity modes. The spacing between modes is ~26 kHz and the bandwidth is ~2.8 kHz, corresponding to quality factors Q of ~300. The maximum reflectivity was ~20 dB. Figure 11(b) shows the theoretical spectrum and it predicts a spacing of ~28 kHz and a Q of ~500. At the resonant frequencies, the acoustic amplitude within the cavity is enhanced by a factor of ~4, compared with the amplitude outside. A calculation of the reflection spectrum of one of the gratings of the cavity is also shown in Figure 11(c), and it predicts a maximum power reflectivity of ~0.93.

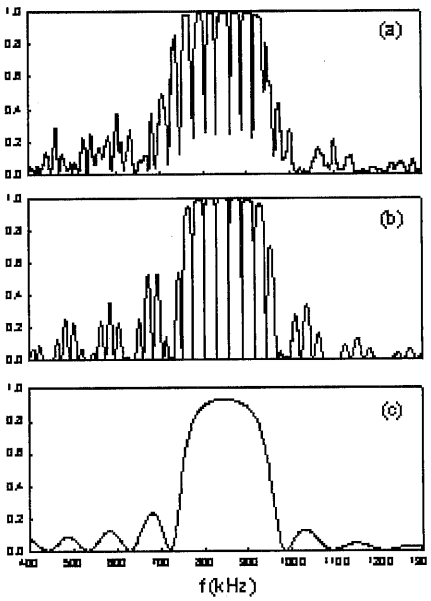

Figure 11. Experimental (a) theoretical (b) graphs of acoustic reflectivity as a function of frequencyfor the acoustic cavity and (c) calculation of the reflection spectrum of one of the gratings forming the cavity

The theoretical and experimental curves are in broad agreement. The small discrepancies are believed to be caused by non-uniformities along the grating, such as small fluctuations of the period and variations of the diameter of the microtapers.

Higher quality factors are achievable by increasing the reflectivity of the gratings, which can be easily done by increasing the number of periods as has been demonstrated for the single acoustic grating. Calculations on similar structures with gratings having 25 periods result in quality factors of ~5×10^5 and amplitude enhancement factors of ~75.

4. CONCLUSIONS

In conclusion, a tapered optical fibre is an ideal medium to study acoustic and acousto-optic interactions, which may lead to some very useful applications. First, we demonstrated an all fibre, tunable, acousto-optic notch filters with bandwidth as small as 2.8 nm. These filters were fabricated from highly uniform tapered single-mode fibre. Because of their all fibre construction, they had a typical excess loss of only 0.02 dB. The filters were widely tunable and polarization insensitive. Then, the acoustic properties of one-dimensional periodic microstructures on optical fibre were experimentally studied, which clearly and unambiguously demonstrate the existence of an acoustic stop band. The flexibility of the fabrication technique readily allows adjustments of the different parameters involved, such as maximum and minimum diameters of the grating and its pitch, thus making feasible modifications of the centre frequency and width of the stop band. Finally, we described and demonstrated a one-dimensional acoustic cavity made on a tapered optical fibre. The cavity was defined by two acoustic Bragg gratings. The modes of the cavity were observed and an experimental Q factor of 300 was measured. Numerical simulations of the reflectivity of the cavity show good agreement with experiment and predict Q factors as high as $5x10^5$ for structures with just 25 periods per grating

5. REFERENCES

[1] D. Ostling, and H. E. Engan, "Narrow-band acousto-optic tunable filtering in a two-mode fibre," *Opt. Lett.*, Vol. 20, pp. 1247-1249, 1995.

[2] H. S. Kim, S. H. Yun, I. K. Kwang, and B. Y. Kim, " All-fibre acousto-optic tunable notch filter with electronically controllable spectral profile," *Opt. Lett.*, Vol. 22, pp. 1476-1478, 1997.

[3] T. A. Birks, P. St. J. Russell, and C. N. Pannell, "Low power acousto-optic device based on a tapered single-mode fibre," IEEE Photon. Technol. Lett., Vol. 6, pp. 725-727, 1994.

[4] T. A. Birks, P. St. J. Russell, and C. N. Pannell, "Four-port fibre frequency shifter with a null taper coupler," *Opt. Lett.*, Vol. 19, pp. 1964-1966, 1994.

[5] S. G. Farwell, M. N. Zervas, and R. I. Laming, "2x2 fused fibre null couplers with asymmetric waist cross sections for polarization independent (<0.01 dB) switching," *J. Lightwave Technol.*, Vol. 16, pp. 1671-1679, 1998.

[6] T. E. Dimmick, G. Kakarantzas, T. A. Birks, and P. St. J. Russell, "Narrow-band acousto-optic tunable filter fabricated from highly uniform tapered optical fibre," in *Proc. OFC`00*, FB4, 2000.

[7] E. Yablonovitch, Phys. Rev. Lett. **58**, 2059 (1987).

[8] M.S. Kushwaha, P. Halevi, L. Dovrzynski and B. Djafari-Rouhani, Phys. Rev. Lett, **71**, 2022 (1993).

[9] E.N. Economou and M. Sigalas, J. Acoustic. Soc. Am., **95**, 1734 (1994).

[10] R. Martinez-Sala, J. Sancho, J.V. Sanchez, V. Gomez, J. Llinares and F. Meseguer, Nature (London) **378**, 241 (1995).

[11] R. James, S.M. Woodley, C.D. Dyer, V.F. Humphrey, J. Acoust. Soc. Am., **97**, 2041 (1995).

[12] M. Shen, W. Cao, Appl. Phys. Lett, **75**, 3713 (1999).

[13] F.R. Montero de Espinosa, E. Jimenez, and M. Torres, Phys. Rev. Lett., **80**, 1208 (1998).

[14] J.V. Sanchez-Perez, D. Caballero, R. Martinez-Sala, C. Rubio, J. Sanchez-Dehesa, F. Meseguer, J. Llinares and F. Galvez, Phys. Rev. Lett., **80**, 5325 (1998).

[15] W.M. Robertson and J.F. Rudy III, J. Acoust. Soc. Am., **104**, 694 (1998).

[16] J.O. Vasseur, P.A. Deymier, G. Frantziskonis, G. Hong, B. Djafari-Rouhani and L. Dovrzynski, J. Phys.Condens. Matter, **10**, 6061 (1998).

[17] B.Y. Kim, J.N. Blake, H.E. Engan, H.J. Shaw, Opt. Lett., **11**, 389 (1986).

[18] T. A. Birks, P.St.J. Russell and D.O. Culverhouse, J. Lightwave Technol. **14**, 2519 (1996).

[19] G. Kakarantzas, T.E. Dimmick, T. A. Birks and P. St.J. Russell , *Opt. Lett.* **26**, N.15, (2001), 1137.

[20] M.V. Andres, M.J. Tudor and K.W.H. Foulds, Electron. Lett., **23**, 774 (1987).

[21] L.M. Brekhovskikh and O.A. Godin, *Acoustics of layered media I, (Springer series on wave phenomena)*, (Springer-Verlag, Berlin 1990).